


## Operator growth in a quantum compass model on a Bethe lattice

X. Zotos 

Department of Physics, University of Crete, 70013 Heraklion, Greece;  
 Foundation for Research and Technology - Hellas, 71110 Heraklion, Greece;  
 and Leibniz Institute for Solid State and Materials Research IFW Dresden, 01171 Dresden, Germany

 (Received 20 November 2020; revised 25 January 2021; accepted 3 May 2021; published 13 May 2021)

The time evolution of local operators in quantum compass models is characterized by simplicity as it can be represented as expanding and contracting strings of operators. Here we present an analytical solution to the problem of growth of a local energy operator in a quantum compass model on a Bethe lattice. We find a linear increase in time of the average operator length and a diffusive spreading of the operator length distribution. Using a moment method, we evaluate the local energy autocorrelation function that shows a Lorentzian shape at low frequencies. Furthermore, using a stochastic method, we visualize the expansion of the string cloud.

DOI: [10.1103/PhysRevB.103.L201108](https://doi.org/10.1103/PhysRevB.103.L201108)

The Bethe lattice [1], due to its distinctive topological structure, offers exact solutions to statistical mechanics problems. In recent years, in studies of quantum chaos, there have been very interesting propositions linking the growth of local operators in quantum many-body systems under unitary dynamics to the emergence of irreversibility and dissipative behavior. Diagnostics such as the out-of-time-order correlator (OTOC) [2] have been extensively studied in a large variety of prototype models [3,4] in search of universal features. The main prediction of these studies is that the operator evolution has a light-cone structure in space-time, while the front broadens diffusively as a function of time. Furthermore, universal properties of operator growth have been proposed [5] as well as a relation of the OTOC to the Loschmidt echo [6].

From another perspective, the dynamics of quantum compass models is an old subject motivated by novel materials with intertwined spin and orbital degrees of freedom [7]. These often two-dimensional quantum magnets are characterized by strongly anisotropic interactions [8] and they have recently been brought back to attention as prototype, fictitious spin models for quantum computing [9].

In this work, we study the time evolution of a local energy operator in a quantum compass model on a Bethe lattice. The key idea of our study is that the operators generated by the time evolution of a local energy operator have a very simple structure, as strings grow and contract on the lattice, i.e., a *discrete quantum branching*. This allows us to analytically evaluate the average size of strings and their distribution as a function of time and, using a moment method, the energy autocorrelation function at infinite temperature. Last but not least, using a stochastic approach, we provide a picture of the expanding *string cloud*.

We study the quantum compass model on a Bethe lattice with threefold coordination, depicted in Fig. 1(a) and given

by the Hamiltonian

$$\begin{aligned}
 H &= \sum_{\langle ij \rangle_x} h_{ij}^x + \sum_{\langle ij \rangle_y} h_{ij}^y + \sum_{\langle ij \rangle_z} h_{ij}^z \\
 &= -J \sum_{\langle ij \rangle_x} \tau_i^x \tau_j^x - J \sum_{\langle ij \rangle_y} \tau_i^y \tau_j^y - J \sum_{\langle ij \rangle_z} \tau_i^z \tau_j^z, \quad (1)
 \end{aligned}$$

where  $\tau^{x,y,z}$  are Pauli pseudospin-1/2 operators and  $J$  is the unit of energy. In Fig. 1(a),  $zz$  represents an initial local energy operator  $O = \tau_0^z \tau_1^z$ . The time evolution  $e^{iHt} O e^{-iHt}$  of this operator is obtained by successive application of the “Liouvillian” operator  $\mathcal{L}$ ,  $\mathcal{L}O = [H, O]$ ,  $\mathcal{L}^2 O = [H, [H, O]]$ , etc. In Figs. 1(b)–1(e), we show examples of different orders  $\mathcal{L}^m$ . For instance, the operator string in Fig. 1(d) is  $\tau_0^z \tau_1^y \tau_2^y \tau_3^x \tau_4^y$  (the numbering of sites is indicative). The key point is the observation that there is no branching of the generated strings and that when a term of  $H$  acts at the middle of a string, it is annihilated [10]. Essentially, the Bethe lattice has the same local bond structure as the honeycomb lattice. Thus the strings that are generated can be easily visualized and accounted for as strings expanding by one leg in four possible directions at their ends or contracting by one leg at either end. It is easy to assign the operator at each node as, by construction, it is the end of the corresponding bond. For instance, in the operator  $\mathcal{L}^2 O$ , there are 24 strings: 4 of length-1 at the origin, 4 of length-1 in the nearest bonds, and 16 of length-3. Thus the evolution of the number  $N_l^{m+1}$  of strings of length  $l$  at the step  $\mathcal{L}^{m+1}$  is given by the simple recursion relation

$$N_l^{m+1} = 2N_{l+1}^m + 4N_{l-1}^m, \quad (2)$$

with the appropriate boundary condition for  $N_1^m$ , as the application of  $\mathcal{L}$  also annihilates a length-1 string. It describes a discrete quantum branching. Numerical iteration of (2) generates  $N_l^m$  to the desired order, but it is also easy (see the Appendix) to obtain an analytical solution.

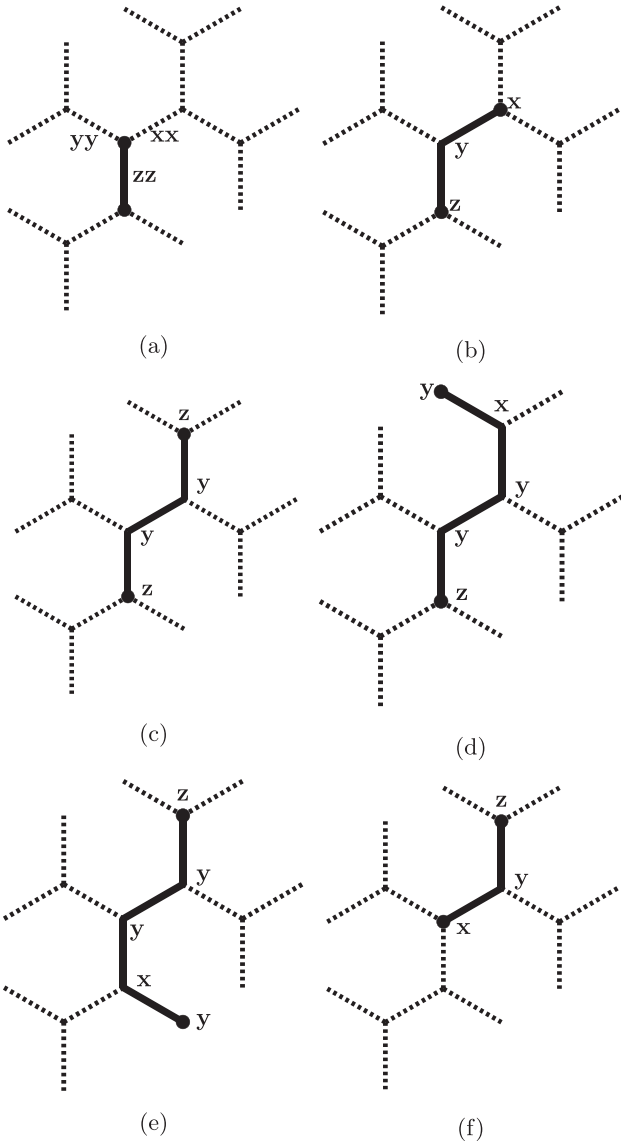


FIG. 1. Example of successive string configurations: (a)  $O = \tau_0^z \tau_1^z$ , (b)  $LO$ , (c)  $L^2O$ , (d)–(f)  $L^3O$ .

The essential features of the expanding string cloud is that (i) after an initial transient of about  $m \sim 20$ , the average length  $\bar{L}_m = \sum_l l P_l^m$  ( $P_l^m = N_l^m / \sum_l N_l^m$ ) increases linearly as a function of Liouville time steps  $m$  with slope  $1/3$ ; (ii) as shown in the inset of Fig. 2, the deviation  $\delta_m = \bar{L}_m - (m/3 + \text{const})$  decreases as a stretched exponential,  $\sim e^{-0.2m^{0.788}}$ ; and (iii) the distribution of lengths  $P_l^m$ , shown in Fig. 3, tends to a Gaussian with width  $\sim \sqrt{m}$  for large  $m$ . The width of the distribution, shown in the inset of Fig. 3, is given by  $\sigma_m^2 = \sum_l (l - \bar{L}_m)^2 P_l^m$ .

Furthermore, the average length as a function of time can be obtained from the moment expansion of the probability distribution,

$$P_l(t) = \sum_{m=0}^{+\infty} \frac{N_l^m}{m!} t^m. \quad (3)$$

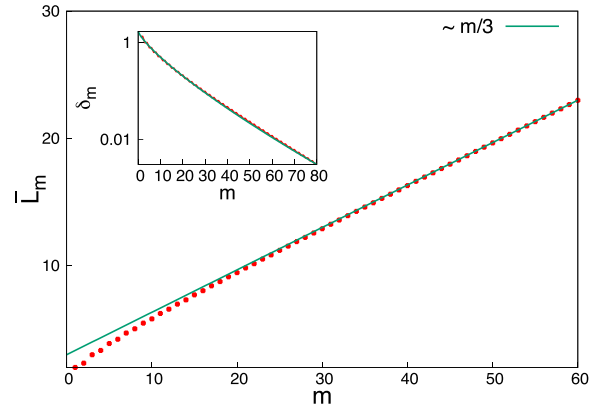


FIG. 2. Time dependence of average string length  $\bar{L}_m$ . Inset:  $\delta_m$  is the deviation from slope  $m/3$ , fitted to a stretched exponential.

The normalized distribution  $P_l(t) = p_l(t) / \sum_l p_l(t)$  gives the average length  $\bar{L}(t) = \sum_l l P_l(t)$ . As shown in Fig. 4, after a transient, the average length of strings,  $\bar{L}(t)$ , grows linearly with time  $t$  with slope 2.

We should note that in the enumeration of generated strings, we do not take into account the minus sign (due to the Pauli pseudospin-1/2 commutation relations) that appears when a string is added to the list of strings of a given configuration, but with “head” and “tail” reversed. We have verified that taking into account these minus signs, appearing to higher iteration order, does not qualitatively change the above operator growth picture.

Next, to correlate the diffusive growth of the operator length distribution to energy transport, we study the frequency dependence of the local energy autocorrelation function,

$$C(t) = \langle O(t)O \rangle, \quad (4)$$

in the infinite temperature limit, on a lattice with  $L$  spins,

$$C(t) = \frac{1}{2^L} \text{tr} O(t)O, \quad (5)$$

from a moment expansion,

$$C(t) = \sum_{m=0}^{\infty} \frac{(-1)^m}{(2m)!} \mu_{2m} t^{2m}, \quad \mu_{2m} = \frac{1}{2^L} \text{tr} O \mathcal{L}^{2m} O. \quad (6)$$

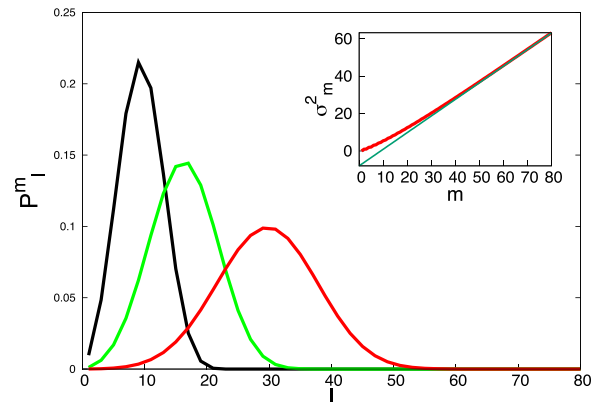


FIG. 3. String length distribution  $P_l^m$ ,  $m = 20$  (black),  $m = 40$  (green),  $m = 80$  (red). Inset: width  $\sigma_m^2$  of distribution  $P_l^m$ .

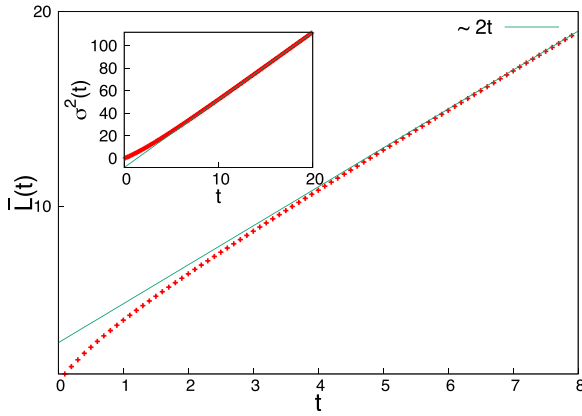


FIG. 4. Time dependence of average string length  $\bar{L}(t)$  as a function of time. Inset: the variance  $\sigma^2(t)$  with slope 6.

As  $O^2 = 1$ , the autocorrelation function reduces to the evaluation of the moments,  $\mu_{2m}$  [11], related to the number  $\bar{\mu}_{2m}$  of strings of length one at the origin after  $m$  Liouville steps. For instance, the second moment is equal to 4, as there are four ways to return to the original string at the origin after  $\mathcal{L}^2 O$ . As we cannot enumerate the moments in an analytical way, we apply a complete generation and accounting of strings generated on a finite Bethe lattice with up to 12 branching steps in each direction. In this calculation, we take into account the minus signs appearing in the generated operators through the process discussed above. Furthermore,

$$S(\omega) = \int_{-\infty}^{+\infty} C(t)e^{+i\omega t} dt \quad (7)$$

is evaluated by an extension to complex frequencies  $z$ ,

$$c(z) = \int_0^{+\infty} C(t)e^{-zt} dt, \quad \text{Re}(z) > 0, \quad (8)$$

$$S(\omega) = \lim_{\eta \rightarrow 0^+} 2\text{Re}[c(\eta - i\omega)], \quad (9)$$

and then  $c(z)$  is conveniently expressed as a continued fraction expansion,

$$c(z) = \frac{1}{z + \frac{\Delta_1}{z + \frac{\Delta_2}{z + \dots}}} \quad (10)$$

The coefficients  $\Delta_n$  are related to the moments  $\mu_{2m}$  by recursion relations [11]. A list of the first 12 moments growing as  $\bar{\mu}_m \sim e^{1.5m}$  and corresponding  $\Delta$  coefficients are given in the table (note that  $\mu_m = 2^m \bar{\mu}_m$ , the factor of  $2^m$  coming from the commutation relation of the Pauli matrices).

$\bar{\mu}_2$	$\bar{\mu}_4$	$\bar{\mu}_6$	$\bar{\mu}_8$	$\bar{\mu}_{10}$	$\bar{\mu}_{12}$
4	44	676	12316	249044	5404780
$\Delta_1$	$\Delta_2$	$\Delta_3$	$\Delta_4$	$\Delta_5$	$\Delta_6$
16.00	28.00	27.43	30.24	29.67	30.96

In Fig. 5, we show  $S(\omega)$  obtained from the continued fraction with a broadening  $\eta = 0.1$  and taking an asymptotic

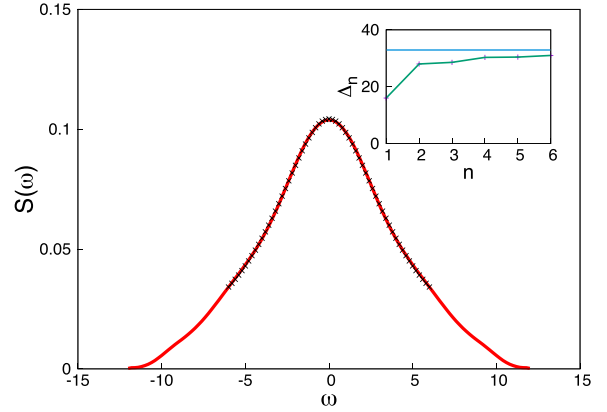


FIG. 5. Autocorrelation function  $S(\omega)$  and a low-frequency Lorentzian fit (black symbols). Inset: coefficients of the continued fraction expansion and an asymptotic.

$\Delta_{n>6} = 33$ . The low-frequency behavior seems to be well fitted by a Lorentzian; further moments are necessary to confirm the diffusive character (although the overall shape does not seem very sensitive to the exact values of the last moments and asymptotic value). It is an interesting issue whether the dissipative energy transport is related to the diffusive spreading of the string lengths' distribution.

As we are dealing with a growth problem, we can apply a stochastic approach to get a picture of the evolution of the string cloud. Starting from the initial  $zz$  bond, by a random choice of direction of expansion or contraction of a string, we stochastically generate a large sample of strings. Their number of a given configuration at each level of iteration is, of course, proportional to their number in the complete evolution of the string cloud. For instance, we can get an estimate of the moment,  $\bar{\mu}_m \simeq N^m \frac{\bar{N}^m}{N_s}$ , from the known total number of strings  $N^m$  at iteration  $m$ , where  $N_s$  is the number in the sample of randomly generated strings after  $m$  iterations and  $\bar{N}^m$  is the number of  $zz$  strings at the origin. Although this estimate, with an error  $O(\frac{1}{\sqrt{N_s}})$ , can be very accurate, we found that it is not sufficient for the evaluation of the  $\Delta_{n>6}$ 's in the continued fraction expansion, as the recursion relations are a highly unstable procedure.

To create the randomly generated strings, we first code the nodes of the Bethe lattice with a pair in coordinates  $(i, j)$ , where  $i$  is the "radial" distance from the origin  $(1,1)$  and  $j$  is the "circular" coordinate, e.g.,  $(1,1)$  is the origin;  $(2,1), (2,2), (2,3)$  are its nearest neighbors;  $(3,1), (3,2)$  are the neighbors of  $(2,1)$ ;  $(3,3), (3,4)$  are the neighbors of  $(2,2)$ ; etc. Thus, the number of nodes at level  $i$  is equal to  $3 \times 2^{i-2}$ . In the Bethe lattice, a string is uniquely defined by the coordinates of the nodes at its two ends,  $(i_b, j_b), (i_e, j_e)$ . Therefore next, in each iteration, we stochastically move one of the two ends in one of the three possible directions.

To study the evolution of the string cloud, we can define an average distance of a string from the origin as  $d = (i_b + i_e)/2$ . In Fig. 6, a picture of the expansion of the string cloud shows the same features as the above analysis of average length growth and distribution. We typically consider about  $10^8$  random string configurations.

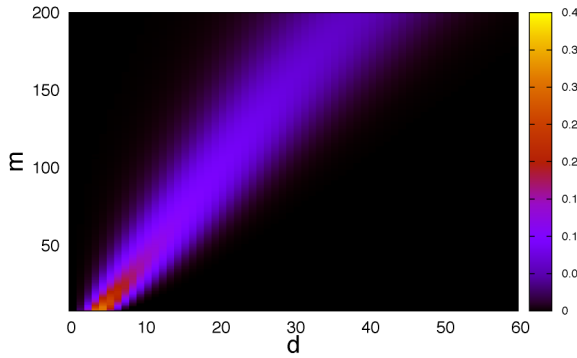


FIG. 6. Color map of the expansion of the string cloud. The color intensity is proportional to the number of strings, normalized to the number of samples, at average distance  $d$  from the origin after  $m$  (for clarity,  $m > 4$ ) iterations. The distance  $d$  is shown in the  $x$  axis; the number of iterations,  $m$ , is shown in the  $y$  axis.

In conclusion, this quantum compass branching model is a paradigm of operator growth. It demonstrates the linear in time evolution of the average length of operator strings, the diffusive spread of strings lengths, and the expansion of the string cloud. The simplicity of the string structure is due to the fully anisotropic compass interactions on the Bethe lattice. Despite this apparent simplicity in the description of the string cloud, a complexity emerges in the distribution of string lengths and positions that leads to a diffusive growth of string lengths. It is an open question whether this complexity implies the diffusive transport that we find in the energy autocorrelation function. The addition of a magnetic field or “bond disorder,” for instance replacing a  $zz$  bond with an  $xx$  bond, only creates side branching. In contrast, the addition of a different type of interaction, e.g., Heisenberg term, destroys the string structure. By the stochastic approach as well as analytical methods, a further study of the operator growth as a statistical mechanics problem should be possible.

This work was supported by the Deutsche Forschungsgemeinschaft through Grant No. HE3439/13.

## APPENDIX

The recursion relation (2) can be seen as the successive application of a tridiagonal Toeplitz matrix  $U$  of dimension  $n$ , with elements  $a = 4$  above the diagonal and  $b = 2$  below, on an initial vector  $N^0 = (1, 0, 0, 0, \dots)^T$ . The right eigenvectors of  $U$  are given by  $|x\rangle_k = \frac{2}{n+1} \sqrt{\frac{a}{b}} \sin \frac{jk\pi}{n+1}$ ,  $j, k = 1, \dots, n$ ; the left ones are given by  $\langle x|_k = \frac{2}{n+1} \sqrt{\frac{b}{a}} \sin \frac{ik\pi}{n+1}$ ,  $j, k = 1, \dots, n$ ; and the corresponding eigenvalues  $\epsilon_k = 2\sqrt{ab} \cos \frac{k\pi}{n+1}$ . Thus the string length vector  $N_l^m$ ,  $l = 1, \dots, m+1$ , obtained from  $U^m N^0 = N^m$ ,  $n > m+1$ , has the components

$$N_l^m = \sum_{k=1}^n \left( 2\sqrt{ab} \cos \frac{k\pi}{n+1} \right)^m \frac{2}{n+1} \left( \frac{b}{a} \right)^{l/2} \times \sin \frac{k\pi}{n+1} \left( \frac{a}{b} \right)^{l/2} \sin \frac{kl\pi}{n+1}. \quad (\text{A1})$$

Taking  $n \rightarrow \infty$ , we obtain

$$N_l^m = \left( \frac{2}{\pi} \right) \int_0^\pi dx (2\sqrt{ab} \cos x)^m \left( \frac{b}{a} \right)^{l/2} \sin x \times \left( \frac{a}{b} \right)^{l/2} \sin(lx). \quad (\text{A2})$$

This expression is nonzero for  $m$  even,  $l$  odd; or  $m$  odd,  $l$  even; and  $l \leq m+1$ . Concretely, for  $m$  even,  $l$  odd,

$$N_l^m = \left( \frac{2}{\pi} \right) (2\sqrt{ab})^m \left( \frac{b}{a} \right)^{l/2} \left( \frac{a}{b} \right)^{l/2} \times \frac{l\pi}{2^{m+1}} \frac{m!}{\left(\frac{m}{2} - \frac{l-1}{2}\right)! \left(\frac{m}{2} + \frac{l-1}{2} + 3\right)!}. \quad (\text{A3})$$

In the limit of large  $m$ , (A3) can be evaluated in the saddle-point approximation,

$$N_l^m \sim e^{-\frac{(l-m/3)^2}{2\sigma^2}}, \quad \sigma^2 = \frac{8}{9}m. \quad (\text{A4})$$

[1] H. A. Bethe, *Proc. R. Soc. London A* **150**, 552 (1935).  
 [2] A. Larkin and Y. N. Ovchinnikov, *Sov. Phys. JETP* **28**, 1200 (1969).  
 [3] D. A. Roberts, D. Stanford, and A. Streicher, *J. High Energy Phys.* **06** (2018) 122.  
 [4] C. W. von Keyserlingk, T. Rakovszky, F. Pollmann, and S. L. Sondhi, *Phys. Rev. X* **8**, 021013 (2018); T. Rakovsky, F. Pollmann, and C. W. von Keyserlingk, *ibid.* **8**, 031058 (2018).  
 [5] D. E. Parker, X. Cao, A. Avdoshkin, T. Scaffidi, and E. Altman, *Phys. Rev. X* **9**, 041017 (2019).

[6] B. Yan, L. Cincio, and W. H. Zurek, *Phys. Rev. Lett.* **124**, 160603 (2020).  
 [7] K. Kugel and D. Khomskii, *Sov. Phys. Usp.* **25**, 231 (1982).  
 [8] Z. Nussinov and J. van den Brink, *Rev. Mod. Phys.* **87**, 1 (2015).  
 [9] A. Yu. Kitaev, *Ann. Phys. (Amsterdam)* **321**, 2 (2006).  
 [10] A. K. R. Briffa and X. Zotos, *Phys. Rev. B* **97**, 064406 (2018).  
 [11] M. Böhm, V. S. Viswanath, J. Stolze, and G. Müller, *Phys. Rev. B* **49**, 15669 (1994).